

ARRANGEMENT OF GRAVEL PILE FOR PREVENTING LIQUEFACTION

By Sukeo O-HARA* and Tetsuro YAMAMOTO**

(Received July 13, 1985)

Abstract

The studies on a gravel pile method used for the prevention of liquefaction of saturated sand deposit during an earthquake have been carried out. To evaluate the pore pressure developed in the sand deposit 20m in depth, in which the gravel pile was installed, we solved the consolidation equation, using the finite difference method.

The radii of the gravel piles 20m in length were taken 0.075, 0.15, 0.25 and 0.40m. The EL Centro earthquake record (NS-Comp., May, 1940) and five others were used as the base motion in these analyses.

As a result, the optimum radius and the optimum distance, of the gravel pile, used in a design was determined in the relationships between the cost of construction and the limited value of pore pressure buildup.

Introduction

A gravel pile method is used as the good prevention of a liquefaction of saturated sand deposit during an earthquake.

Though experimental and theoretical studies on the gravel pile method have been performed by several investigators (Seed et al.¹), Ishihara et al.²), Tanaka et al.³), and O-hara et al.^{4,5}), the design standard of the gravel pile method has not yet been established.

In our previous paper⁴), the pore pressure developed in the sand deposit (20m in thickness) installed the gravel pile was calculated and we made clear that the effect of a gravel pile on the prevention of liquefaction extends to 1.25m from a center of a gravel pile.

Although the sinusoidal acceleration wave having the constant amplitude was used in our previous analysis⁴), the EL Centro earthquake record (NS-Comp., May, 1940) and five others were used as the base motion in this analysis.

In order to determine the radius of the affected area of a gravel pile, the maximum pore pressures developed in the saturated sand deposit were investigated. Next, the limited value of pore pressure buildup which don't liquefy the deposit, was decided and the number of gravel piles per unit area, which necessitate to restrain the maximum pore pressure under the aboved limited value, was determined. Finally, the optimum radius and optimum distance, of the gravel pile were determined by minimizing the cost of construction of gravel pile.

* Department of Civil Engineering

** Department of Civil Engineering, Technical Junior College, Yamaguchi University

Analysis

Because the sand deposit and the procedure of analysis were the same as that of our previous paper⁴⁾, we shall describe them only briefly in this paper.

The saturated sand deposit and the physical properties of sand, used in this analysis are shown in Fig. 1.

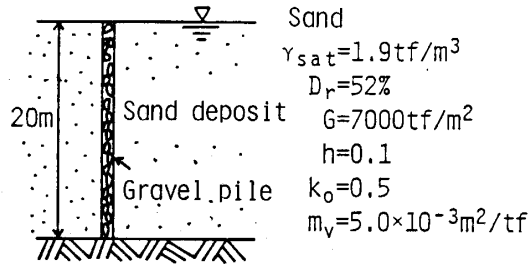


Fig. 1 Sand deposit used in this analysis.

It was assumed that a ground water level is equal to the surface of sand deposit and the sand deposit is 20m in thickness.

In this analysis, the width of deposit was changed every 1.0m in the region of 1.0m ~ 6.0m, to investigate the radius of affected area of a gravel pile. The calculations were performed for a radius of gravel pile $r_g = 0.075\text{m}$, 0.15m , 0.25m and 0.40m and it was assumed that the length of gravel pile is 20m.

These calculations were performed by the finite difference method. The lengths in the radial and vertical directions of elements (Δr , Δz) are both the same as $1/6\text{m}$. The increment of time is 0.005sec .

Because assuming the flow of pore water was governed by Darcy's Law and the thickness of deposit was considerably larger than it's width, the vertical flow of pore water could be neglected.

Therefore, assuming the coefficient of permeability in vertical direction $k_v = 0\text{m/s}$, we obtained the pore pressure developed in the saturated sand deposit using the two-dimensional consolidation Eq. (1). The boundary conditions are indicated by Eq. (2).

The difference of calculated results between for $k_v = 0\text{m/s}$ and $k_v \neq 0\text{m/s}$ was not recognized.

$$c_v \cdot \left(\frac{\partial^2 u}{\partial r^2} + \frac{1}{r} \cdot \frac{\partial u}{\partial r} \right) = \frac{\partial u}{\partial t} \quad (1)$$

$$\left. \begin{array}{l} (u)_{r=r_g} = 0 \\ (\partial u / \partial r)_{r=r_0} = 0 \end{array} \right\} \quad (2)$$

Where $c_v (= k_H / m_v \cdot \gamma_w) =$ coefficient of consolidation, $k_H =$ coefficient of permeability in horizontal direction, $m_v =$ coefficient of volume compressibility, $\gamma_w =$ unit weight of water, $t =$ time, $r_g =$ radius of gravel pile, $r_0 =$ distance between the center of gravel pile

and outer circle of the cylindrical sand deposit.

The shear stress developed in the sand deposit was calculated from Eq. (3), using Newmark's β -method.

The equation (3) was deduced by modeling the sand deposit to the lumped mass system.

$$M \cdot \ddot{u}(t) + C \cdot \dot{u}(t) + K \cdot u(t) = -M \cdot \ddot{u}_g(t) \quad (3)$$

where M = mass matrix, C = damping matrix, K = stiffness matrix, u = displacement vector, \ddot{u}_g = acceleration vector.

The damping matrix C is obtained using the following equation : $C = h \cdot \omega_1 [M] + h / \omega_1 [K]$, where h indicates the damping factor and was assumed $h = 0.1$, ω_1 indicates the first natural circular frequency and it depends on the shear modulus.

ω_1 of this deposit was 14.917 rad/s.

The earthquake records used in this analysis are summarized in Table 1. Also, the white noise was used in addition to these records.

Table 1 Earthquake records.

Name of wave	Date	Comp.	Max. Acc.(gal)
EL Centro	1940.5.18	N—S	326.0
Taft	1952.7.21	N21E	152.7
Hachinohe	1968.5.16	N—S	232.7
Niigata	1964.6.16	E—W	156.9
Kaihokubashi	1978.6.12	Tr	286.8

The maximum amplitudes of acceleration of every waves were made up to 100gal at calculations.

We calculated the change of pore pressure by the following procedure : first, the vertical distributions of maximum shear stress induced during first half period of first cycle (number of cycle (n) = 1) and this half period were obtained. Thereafter, pore pressure induced at $n = 1$ was obtained using Eq. (1), by applying the pore pressure u_a given by Eq. (4) to Eq. (1) as the initial value. Similarly, the maximum shear stress induced during secondary half period of first cycle ($n = 2$) and this secondary half period were obtained. Substituting the shear stress at $n = 2$ and coefficient of pore pressure decrease ($\Delta u/\bar{u}$) at $n = 1$ into Eq. (5), the pore pressure u_a was obtained. Moreover, applying the sum of this u_a and previous pore pressure into Eq. (1) as new initial value, the increment of pore pressure at $n = 2$ was obtained from Eq. (1).

The same calculation was repeated successively, to obtain the increment of pore pressure at after $n = 3$.

More, Eq. (4) and Eq. (5) indicated the rate of pore pressure increase and were obtained from the series of cyclic triaxial tests carried out under partial drained condition. The detailed procedure is explained in previous paper⁴.

$$u/\sigma_3 = 1.005 \cdot (\sigma_d/2\sigma_3) - 0.0931 \quad (n=1) \quad (4)$$

$$u/\sigma_3 = \left[\{-0.0805 \cdot (\Delta u/\bar{u}) + 0.0378 + 0.7273 \cdot e^{-1000 \cdot (\Delta u/\bar{u})}\} \cdot (\sigma_d/2\sigma_3) + \right. \\ \left. \{0.0092 \cdot (\Delta u/\bar{u}) - 0.0030 - 0.0823 \cdot e^{-1000 \cdot (\Delta u/\bar{u})}\} \cdot n + 0.2400 \cdot (\sigma_d/2\sigma_3) - \right. \\ \left. 0.0079 \right] \quad (n \geq 2) \quad (5)$$

where σ_d = cyclic deviator stress, σ_3 = cell pressure, u = pore pressure, Δu = amount of pore pressure decrease, \bar{u} = pore pressure before the decrease occurs.

Because the amount of pore pressure buildup was obtained for every half period in this analysis, Eq. (4) and Eq. (5) were changed to make their calculated values equal to half of previous values⁴⁾.

Eq. (6) should be used when the pore pressure developed in the sand deposit is obtained using Eq. (4) and Eq. (5).

$$\left. \begin{aligned} \sigma_3 &= \frac{1 + 2K_o}{3} \sigma_v \\ (\sigma_d/2\sigma_3) &= \frac{3}{1 + 2K_o} (\tau/\sigma_v) \end{aligned} \right\} \quad (6)$$

where σ_v = effective vertical stress, τ = cyclic shear stress, K_o = coefficient of earth pressure at rest.

Pore Pressure Developed in Saturated Sand Deposit Installed Gravel Pile

In this paper, the amount of pore pressure buildup and its vertical distribution developed in the deposit which gravel piles were installed, were investigated.

Fig. 2 indicates the relationships between the pore pressure ratio (u/σ_v) and the earthquake duration (t), at depth $z = 6.0\text{m}$, which were obtained for $r_o = 1.25\text{m}$ and $r_g = 0.25\text{m}$.

It may be seen in Fig. 2 that the distinct difference of the amount of pore pressure buildup depends on the earthquake records.

When Taft record and Hachinohe record were used as base motion, the liquefaction of deposit occurred (u/σ_3 has attained to 1.0) and conversely, when the other records were used, the liquefaction of deposit did not occur.

Fig. 3, Fig. 4 and Fig. 5 show the time histories of cyclic shear stresses at depth $z = 6.0\text{m}$ which was developed in the deposit under three base motions: Taft record, Niigata record and white noise, respectively. The Niigata record was obtained at base-ment of Kawagishi-cho-apartment and is affected considerably by the liquefaction of deposit.

It is clear from Fig. 2, Fig. 3, and Fig. 4 that the amount of pore pressure buildup developed in the deposit is proportional to shear stress induced in the deposit. Fig. 6 shows the effect of permeability of deposit on the amount of pore pressure buildup developed in the deposit. This results shown in Fig. 6 were obtained for EL Centro earthquake record. The natural deposits usually liquefy without reference to the permeability

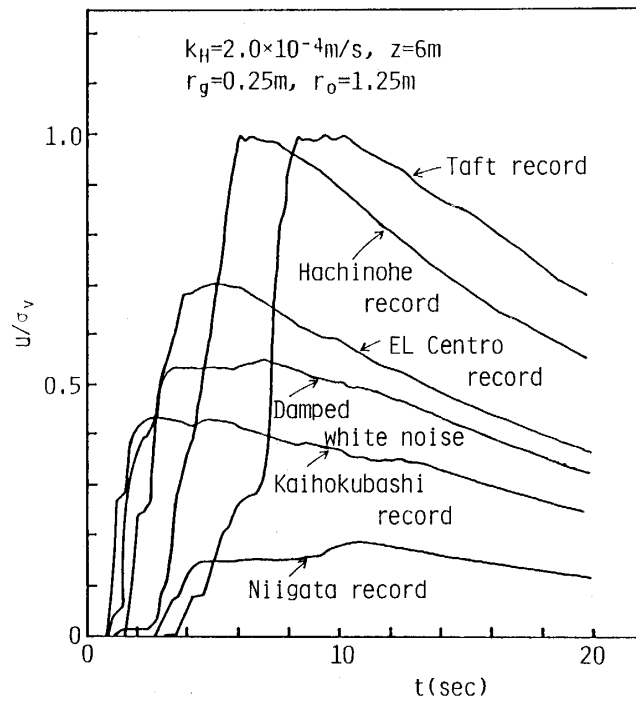


Fig. 2 Pore pressure buildup curves.

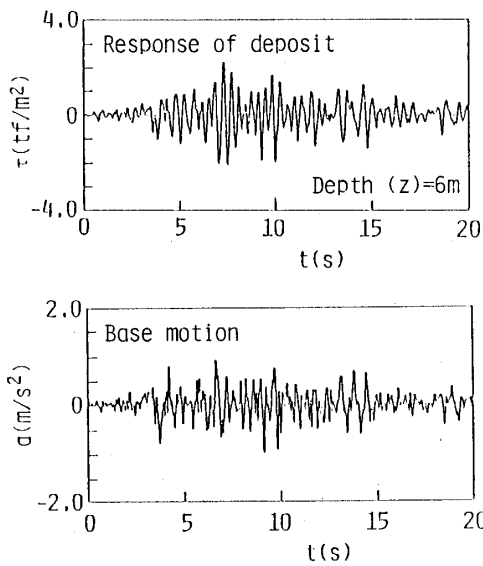


Fig. 3 Base motion and response of deposit (Taft record).

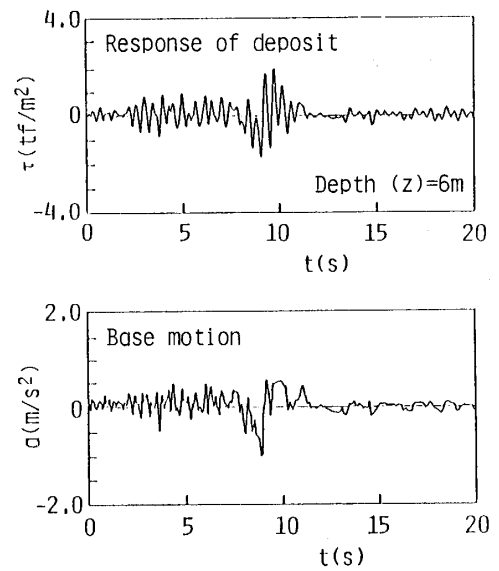


Fig. 4 Base motion and response of deposit (Niigata record).

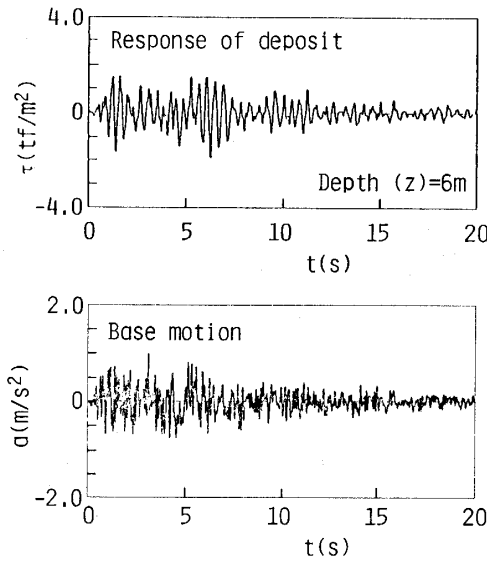


Fig. 5 Base motion and response of deposit (Damped white noise).

of the deposit.

The deposit installed the gravel pile does not liquefy for $k_H = 2.0 \times 10^{-4} \text{m/s}$ and $2.0 \times 10^{-3} \text{m/s}$, except for $k_H = 2.0 \times 10^{-5} \text{m/s}$. The rate of pore pressure decrease is in proportion to the coefficient of permeability of the deposit.

Fig. 7 indicates the vertical distributions of the pore pressure ratios at states which the deposit liquefied or pore pressure attained to maximum.

In this calculations, EL Centro record was used as base motion and also three coefficients of permeability were used. It may be seen from Fig. 7 that the vertical distributions of pore pressure developed in the deposit depend on the coefficient of permeability.

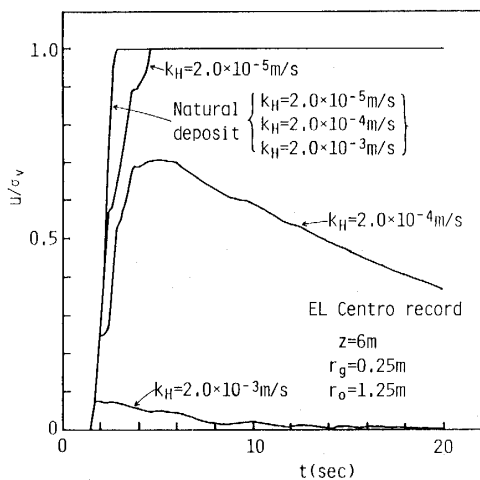


Fig. 6 Effect of permeability of deposit on pore pressure buildup (EL Centro record),

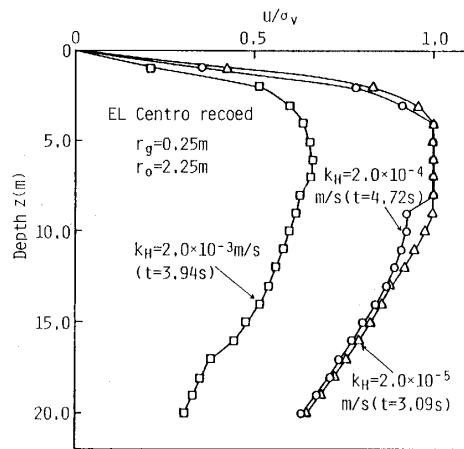


Fig. 7 Vertical distribution of maximum pore pressure ratio.

Investigation on Optimum Dimensions of Gravel Pile

In order to determine the optimum dimensions (radius and installed distance) of the gravel pile, the maximum pore pressure ratio $(u/\sigma_v)_{\max}$ developed in the deposit was calculated using previous earthquake records as the base motion. The radii of gravel pile (r_g) were taken 0.075m, 0.15m, 0.25m and 0.40m and the width of deposit were changed every 1.0m in the region of 1.0m~6.0m.

Fig. 8 shows the relationships between $(u/\sigma_v)_{\max}$ and r_o obtained for respective radii of gravel pile, using EL Centro record. k_H was taken 2.0×10^{-5} m/s, 2.0×10^{-4} m/s and 2.0×10^{-3} m/s, respectively.

As may be seen in Fig. 8, the greater r_g and k_H , the greater r_o become for a constant

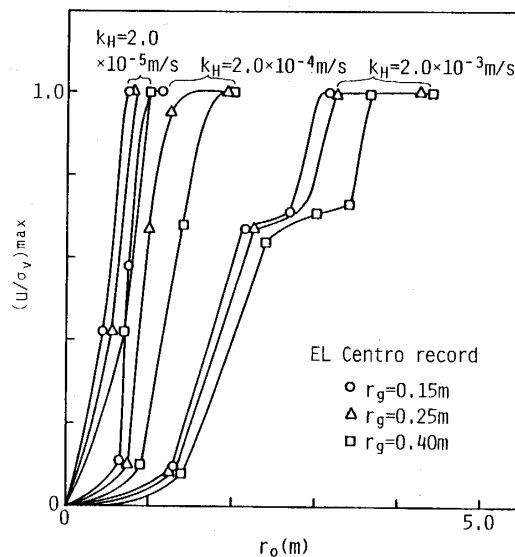


Fig. 8 Relationships between $(u/\sigma_v)_{\max}$ and r_o (EL Centro record).

of $(u/\sigma_v)_{\max}$, i.e. the effect of gravel pile on the pore pressure decrease becomes remarkable in the case of which r_g and k_H are large, because the amount of pore water flowed into the gravel pile increases in proportion to r_g and k_H .

The limited value of $(u/\sigma_v)_{\max}$ should be pre-determined in design of gravel pile but we have yet no authority for the pre-determination of the limited value. For example, Ishihara et al.²⁾ adopted 0.4 as the limited value of $(u/\sigma_v)_{\max}$ when the earthquake duration not exceed 30 seconds.

We considered from our liquefaction test results of saturated sand that the strain of specimen began to rapid increase at $(u/\sigma_v)_{\max} = 0.6 \sim 0.7$ and at this time, the applied shear stress was over the shear strength of saturated sand. So that we first investigated on the optimum dimensions of gravel pile for the case of $(u/\sigma_v)_{\max} = 0.6$. In adding to these investigations, the investigations were performed for the cases of $(u/\sigma_v)_{\max} = 0.8, 0.9$ and 1.0.

The relationships between r_g and r_o were obtained for $(u/\sigma_v)_{\max} = 0.6, 0.8, 0.9$ and 1.0 (Fig. 9). r_o is radius of affected area of a gravel pile.

Using r_o obtained, the cost of construction of gravel pile system was calculated for case which were installed gravel piles, 20m in length, with distance d_e in the square ground 10m in the length of the side, where d_e is equivalent radius and becomes equal to $1.77r_o$ as shown in Fig. 10. The items of direct cost which were used in calculation of

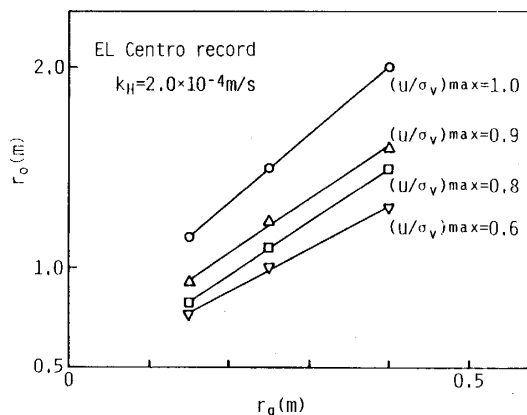


Fig. 9 Relationships between r_o and r_g (EL Centro record).

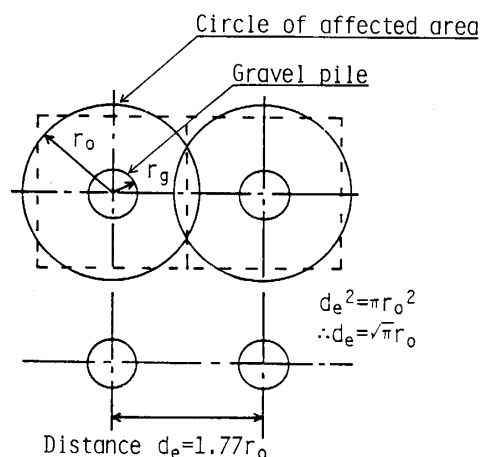


Fig. 10 Radius and distance of gravel pile.

the cost construction, were shown in Table 2. We assumed that the grain size of gravel used in this construction is in the region of 20mm~50mm and the cost of construction is 1.5 times the direct cost.

Table 2 Direct costs of construction of gravel pile.

Radius of gravel pile (mm)	Dray expense (yen/m)	Material expense (yen/m ³)	Packing expense (yen/m ³)
75	20000	2500	1000
150	22000	2500	1000
250	26000	2500	1000
400	45000	2500	1000

Fig. 11 (a) and Fig. 11 (b) indicate the relationships between the cost of construction and r_g for the cases of $(u/\sigma_v)_{\max} = 0.6$ and 1.0 , respectively.

These relationships were obtained for each earthquake record and for $k_H = 2.0 \times 10^{-4} \text{m/s}$.

It is clear from Fig. 11 that the cost of construction depends on the earthquake record and $(u/\sigma_v)_{\max}$ and the certain value of r_g minimizes the cost of construction.

We determined that this certain value of r_g is the optimum radius of gravel pile.

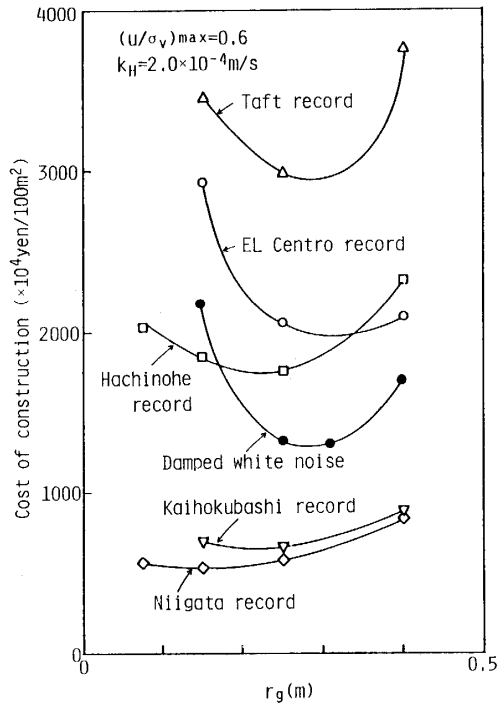


Fig. 11(a) Relationships between cost of construction and radius of gravel pile for $(u/\sigma_v)_{max} = 0.6$.

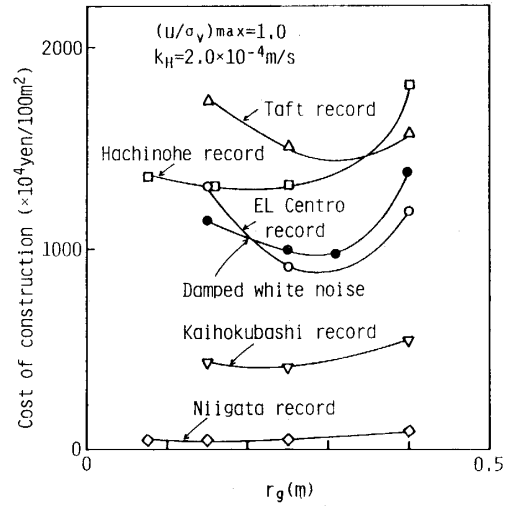


Fig. 11(b) Relationships between cost of construction and radius of gravel pile for $(u/\sigma_v)_{max} = 1.0$.

Fig. 12 shows the relationships between the optimum radius of gravel pile and the limited value of $(u/\sigma_v)_{max}$ for each record.

We may conclude from Fig. 12 that the optimum radius of gravel pile is in the region of 0.2~0.3m independent of the limited value of $(u/\sigma_v)_{max}$.

Now, it was seen from Fig. 11 that the cost of construction depends to the kinds of earthquake records and Taft record maximizes the cost of construction of gravel pile. So that, we considered from the results described above that the calculation using Taft record should be adopted in the design of gravel pile, if the calculation were performed using previous earthquake record.

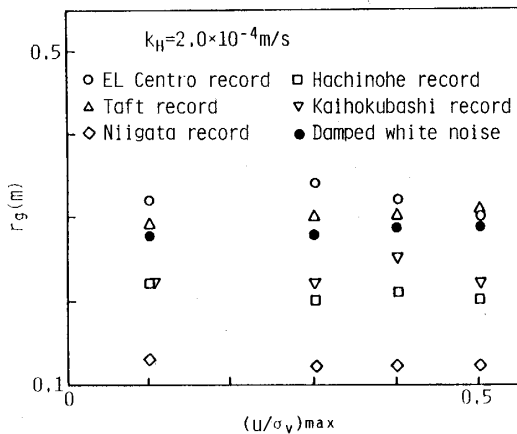


Fig. 12 Relationships between r_g and $(u/\sigma_v)_{max}$.

Design of Gravel Pile Method

Because the characters of previous earthquake records are affected to some degree by the difference of their propagation paths, it is desirable that more universal wave is used in design calculation of gravel pile method. For this reason, we used the damped white noise (white noise with damped amplitude) in this analysis and compared these results with results obtained using earthquake records. These results have been previously shown with the other in Fig. 2, Fig. 5, Fig. 11 and Fig. 12.

It was seen in these figures that the results calculated using the damped white noise were medium between results which were obtained using earthquake records.

Fig. 13 indicates the relationships between r_o and r_g obtained using the damped white noise as the base motion.

The relationships between the cost construction of gravel pile for 100m^2 in area and r_g , given from Fig. 13, were shown in Fig. 11 (a) and Fig. 11 (b).

We can find r_g for the minimum cost of construction from Fig. 12, if we decide the limited value of $(u/\sigma_v)_{\text{max}}$. As may be seen in Fig. 12, it is clear that r_g for the minimum cost of construction is independent of the limited value of $(u/\sigma_v)_{\text{max}}$, i.e. the cost of construction is minimized for $r_g \doteq 0.3\text{m}$ when $k_H = 2.0 \times 10^{-4}\text{m/s}$.

The above mentioned fact is supported by the results obtained using earthquake records.

We can obtain r_o from the optimum radius of gravel pile r_g which is obtained in the procedure described above (Fig. 13).

The relationships between the optimum radius (r_g) and the optimum distance of gravel pile $d_e (= 1.77r_o)$ can be found in Fig. 14, if the limited value of $(u/\sigma_v)_{\text{max}}$ is decided.

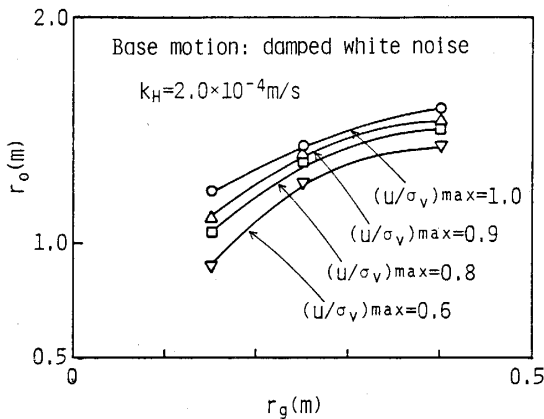


Fig. 13 Relationships between r_o and r_g .

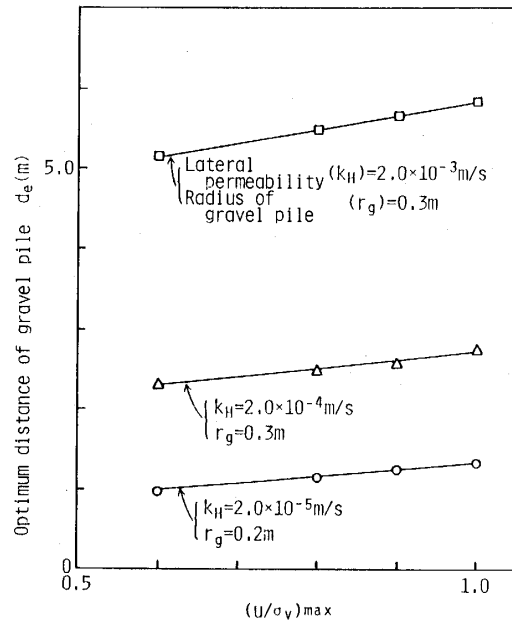


Fig. 14 Optimum radius and optimum distance of gravel pile.

Conclusion

The gravel pile method for the prevention of liquefaction of the saturated sand deposit during an earthquake is studied. In this paper, the optimum radius and the optimum distance of gravel pile were determined in the relationships between the cost of construction and the limited value of pore pressure ratio.

In this analysis, the pore pressures developed in the saturated sand deposit installed gravel pile were calculated and the number of gravel pile per unit area, which necessitate to restrain the pore pressure under the limit, was determined. Finally, the cost of construction was calculated for every case, in order to determine the optimum radius and the optimum installed distance of gravel pile.

Five previous earthquake records and the damped white noise (white noise with damped amplitude) were used as the base motion in these analyses. The latter was used in order to investigate whether the results obtained using the former are universally or not.

The summary of the results is as follows :

- (1) The optimum radii of gravel pile were 0.2~0.35m for E1 Centro record, 0.1m for Niigata record and a medium value 0.3m for the white noise.
- (2) The optimum radii and the optimum installed distance of gravel pile method for shear modulus of deposit $G = 7000\text{tf/m}^2$, and for the coefficient of permeability in horizontal direction of deposit $k_H = 2.0 \times 10^{-5}\text{m/s}$, $2.0 \times 10^{-4}\text{m/s}$ and $2.0 \times 10^{-3}\text{m/s}$ respectively, were indicated in Fig. 14.

Acknowledgments

The authors wish to thank Professor S. Kotsubo at Kyushu University for his useful suggestions and Miss S. Kuroda for her useful help.

References

- 1) Seed, H. B. and Booker, J. R. : Stabilization of Potentially Liquefiable Sand Deposit Using Gravel Drain, Proc. ASCE, Vol. 103, No. GT7, 757-768 (1977)
- 2) Ishihara, K., Saito, A., and Arai, H. : Applying Crushed Stone Piles as a Solution to Liquefaction Problem of Revetment, Tsuchi-to-Kiso, Vol. 28, No. 4, 9-15 (1980) (in Japanese)
- 3) Tanaka, Y., Kokusho, G., Esashi, Y., and Matsui, I. : On Preventing Liquefaction of Level Ground Using Gravel Piles, Proc. JSCE, No. 352, 89-98 (1984) (in Japanese)
- 4) Yamamoto, T., O-hara, S., and Kotsubo, S. : Fundamental Study on Gravel Pile Method for Preventing Liquefaction, Technology Reports of the Kyushu University, Vol. 58, No. 3, 181-189 (1985 (a)) (in Japanese)
- 5) O-hara, S., Kotsubo, S., and Yamamoto, T. : Pore Pressure Developed in Saturated Sand Subjected to Cyclic Shear Stress under Partial Drainage Conditions, Soils and Foundations, Vol. 25, No. 2, 45-56 (1985 (b))